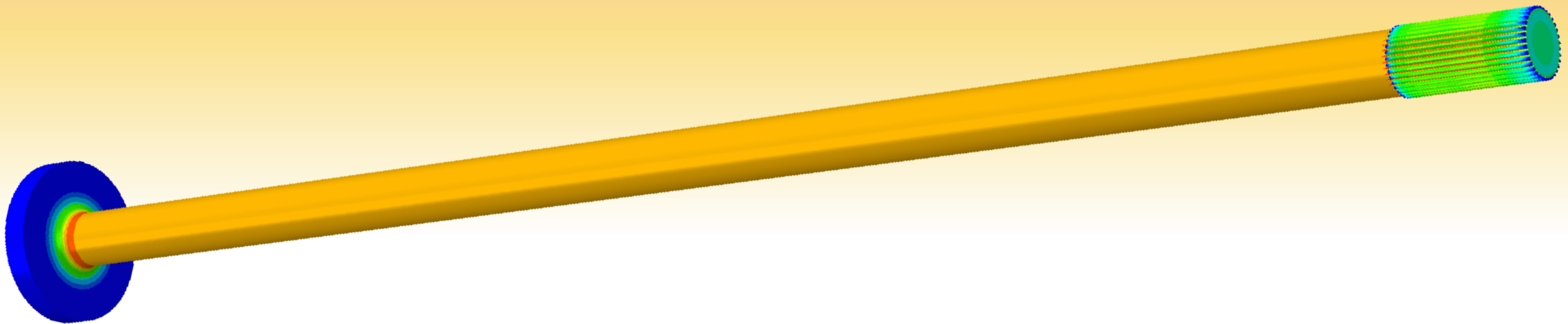




Scanning Induction Hardening of a Truck Axle

Effect of spray quenching and steel hardenability on stress formation and distortion



Axle shafts are typically case hardened using an induction process by rapidly heating to the material's austenitizing temperature through the desired case depth. The shaft is then quenched to form martensite, leaving the surface harder than the base material and under a desirable, compressive residual stress state. The design of inductors can come in several different configurations, depending on part geometry and desired case depth. Predicting the final stress state and overall size change from this process is important in order to ensure the desired performance specifications are met and costs from waste, or scrap, from damaged or highly distorted parts are reduced. Using the DANTE heat treatment simulation software, it is possible to predict the in-process and final stress, displacement, metallurgical phase fractions, and hardness of an induction hardening process in order to tailor the process to achieve the desired results.

In this study, a full-float truck axle, manufactured by Dana Corporation, is chosen as a typical shaft undergoing an induction hardening process. First, a baseline model will be defined in order to have something to compare process modifications to. Next, the effect of changing the quench rate on the final stress state and distortion will be examined. Finally, the effect of changing the hardenability of the material, by altering chemistry and carbon level, on the final stress state will be explored.

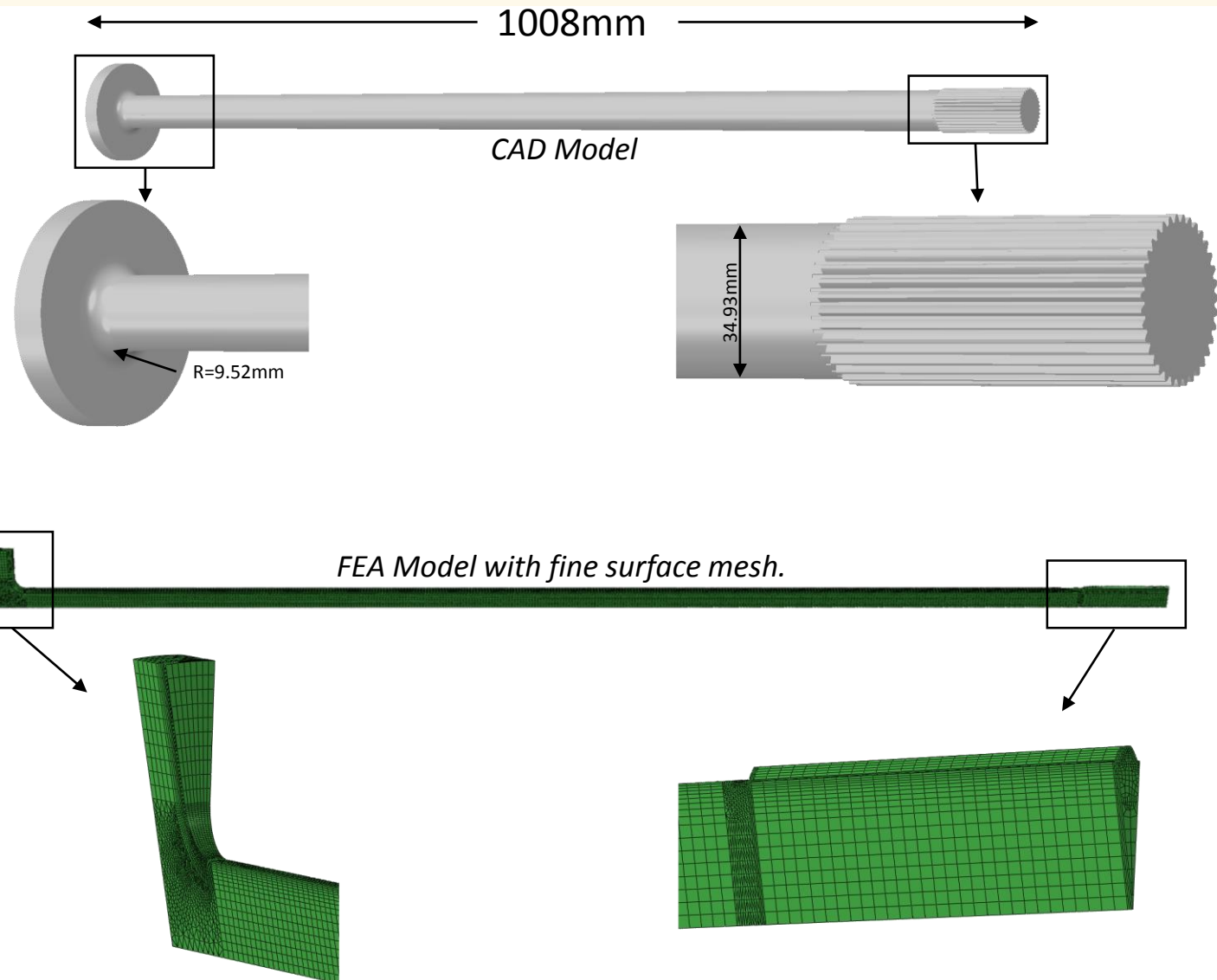
Model Definition

Part:

- 1,008 mm long
- 34.93 mm diameter
- Flange on one end, 35-tooth spline on other end

Model:

Using symmetry, the FEA model will be a slice down the length of the shaft and cover an angle equivalent to one spline tooth. The part is then meshed with very fine surface elements in order to catch thermal and stress gradients present in the process.

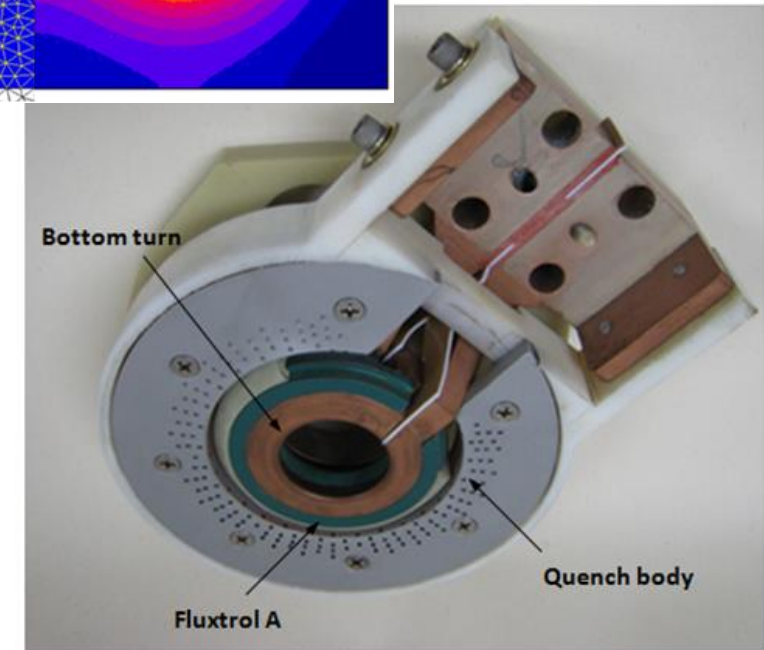
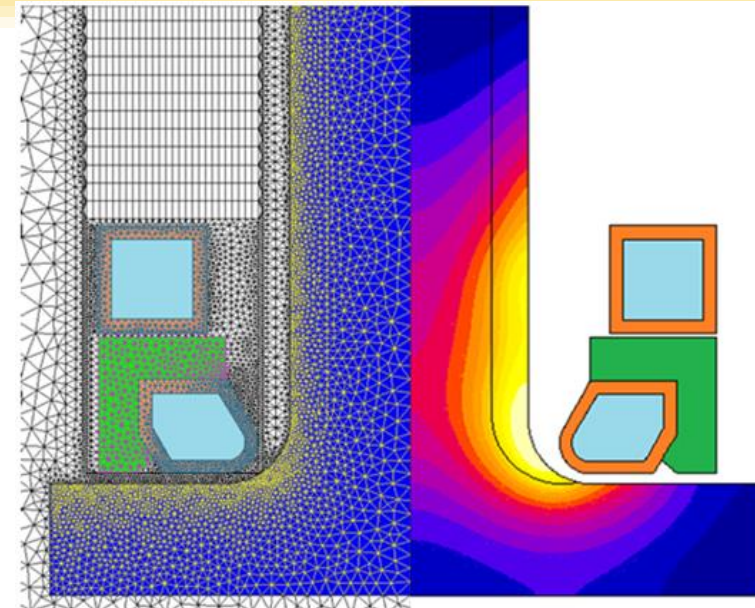


Inductor Definition & Process Outline

The top figure shows the Flux2D® model* used to model the electromagnetic phenomenon, with the inductor in the starting position. The bottom figure is a picture of the inductor used in the actual process.

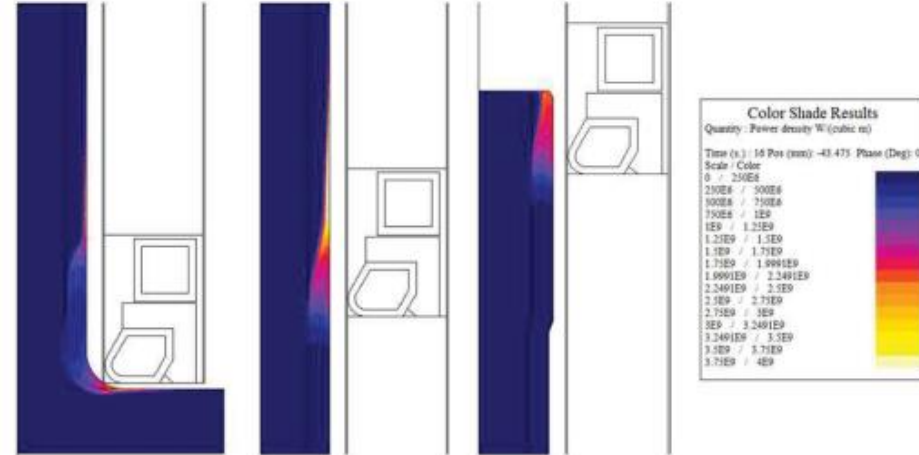
A 2-turn coil was chosen and configured using Flux 2D software to meet the required case depth and model the following process:

1. The inductor dwells at the flange end for 9 seconds to allow heat to build up.
2. The inductor moves up the shaft at a rate of 12 mm/s for 1.5 seconds.
3. The inductor slows to 8 mm/s and spray quenching begins following the heated region. The inductor stops just short of the spline to prevent overheating.
4. After the inductor is shut off, the spline end is allowed to air cool for 60 seconds, for a total process time of 190.15 seconds.

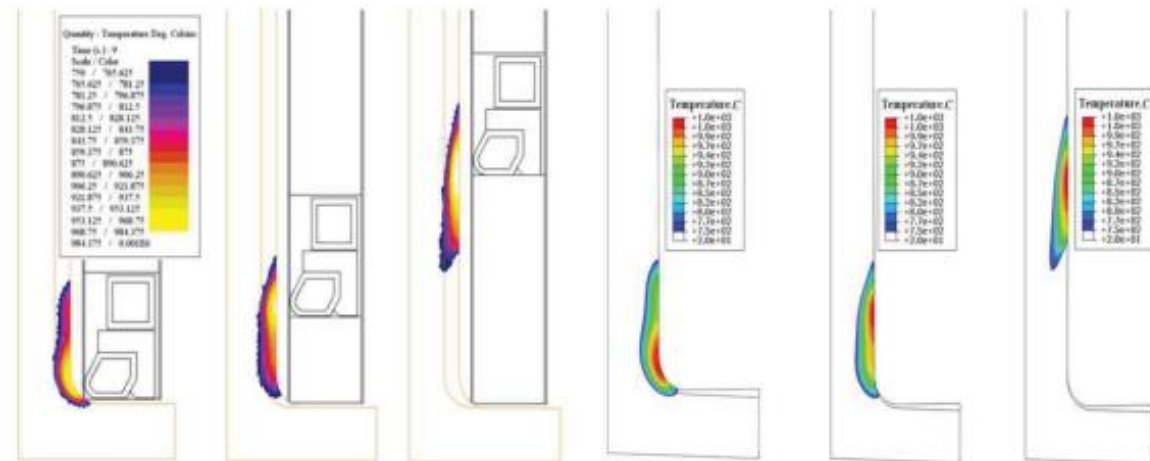


Flux2D to DANTE model validation

- The upper figure shows the power density distribution at several snapshots in time predicted by the Flux 2D software.
- Flux 2D data is imported into the DANTE software as power density versus time for the entire model to provide data to drive a DANTE thermal model of the symmetrical slice of the axle.
- The lower figure shows the Flux 2D temperature prediction compared to the DANTE temperature prediction using the power density versus time data from Flux 2D. The models agree well.
- DANTE thermal and stress models are built with the process parameters in order to analyze the stress distribution and overall change in displacement when the quench rate and material chemistry are changed.



Flux 2D Power Density Distribution



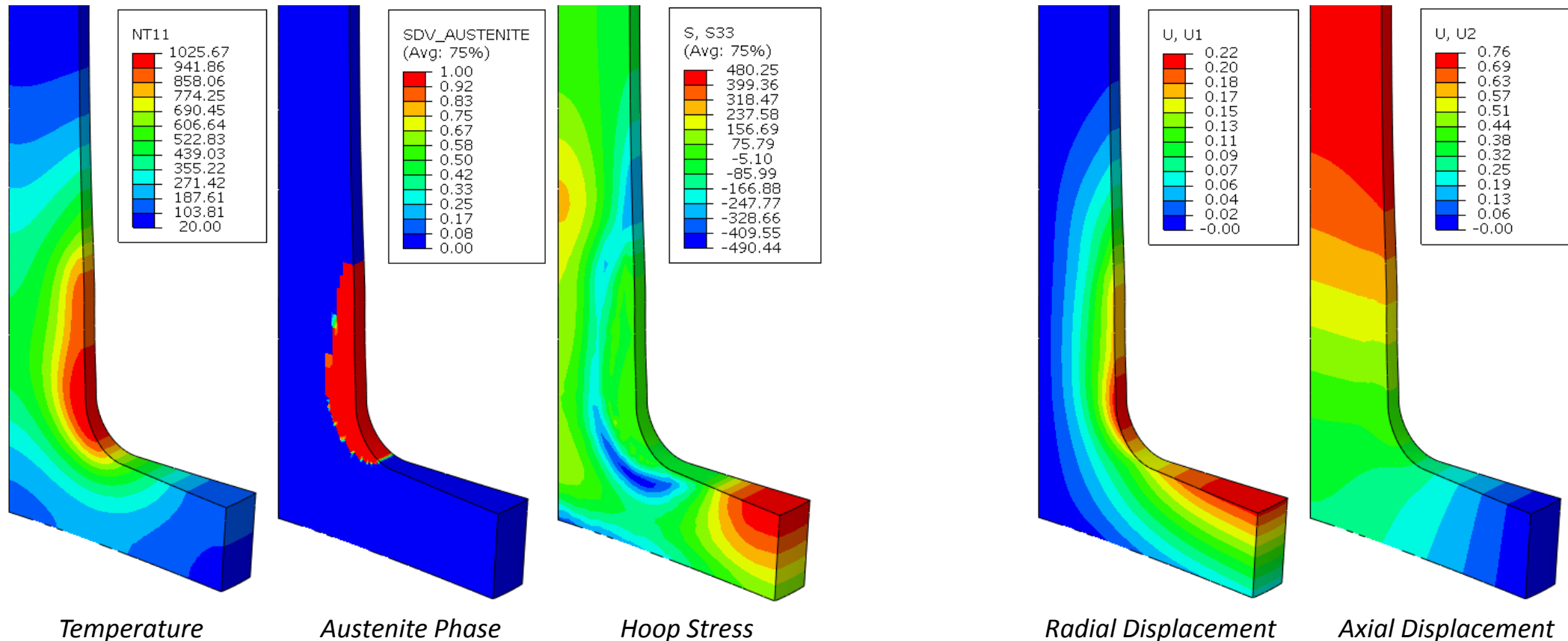
Flux 2D Predicted Temperature

DANTE Thermal Model

Stress, Phase, and Displacement After Initial Dwell

Baseline - AISI 1541 – 25K W/(m²·°C) HTC

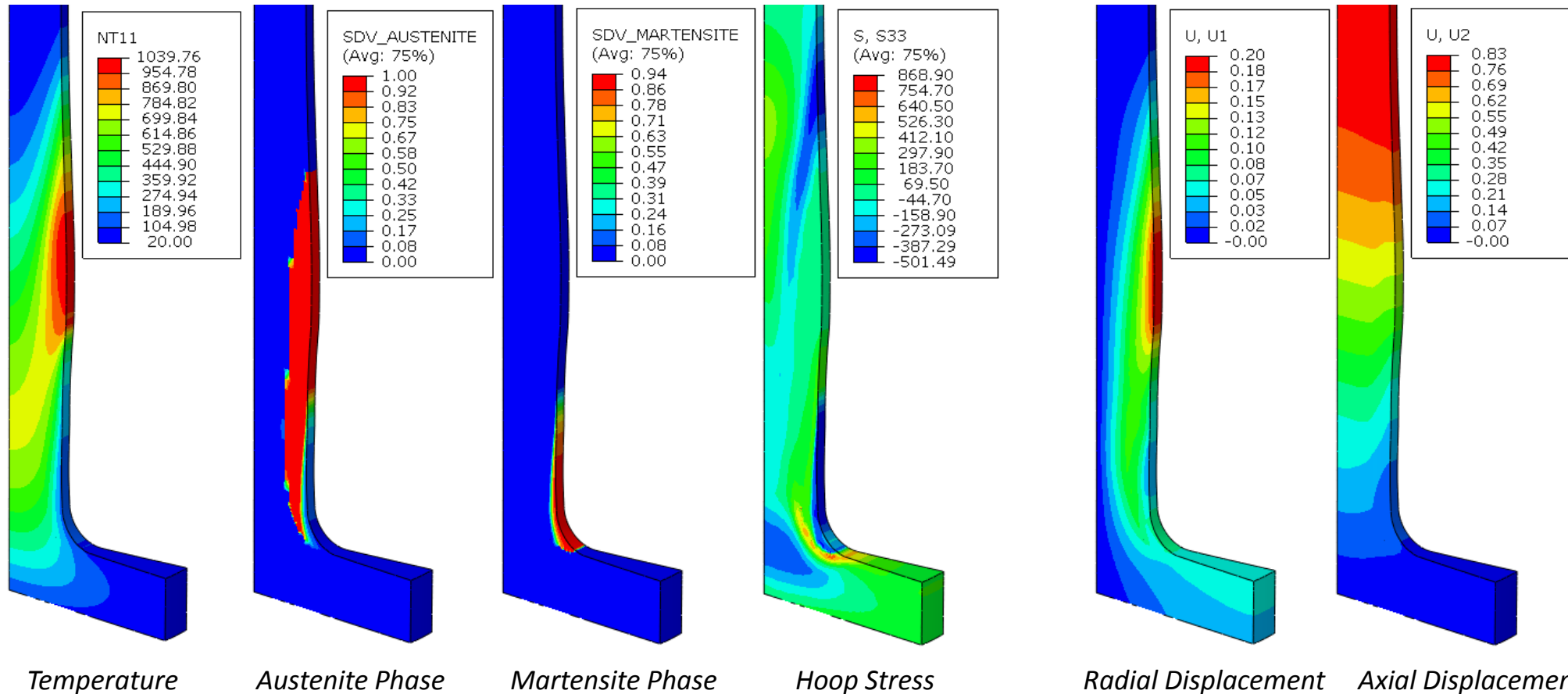
At the end of the 9 second initial dwell, the surface temperature in the flange fillet reaches ~1025°C. Austenite has formed in the fillet, and part way up the shaft. Hoop stress shows compression just under the fillet in the flange from the volume shrinkage on the surface as the initial phase transforms to austenite. Tension is present in the core, just ahead of the heated zone. Displacement on the right shows some radial and axial growth due to thermal expansion.



Stress, Phase and Displacement in Process

Baseline - AISI 1541 – 25K W/(m²·°C) HTC

16.5 sec into the entire process, the inductor is moving upwards at a rate of 8 mm/s, with the quench spray following. The austenite phase is rapidly quenched to form martensite in the flange-fillet and above, causing compression from the volume expansion of the martensite phase, as seen in the hoop stress contour. Tension resides just under the martensite layer as a result of the phase transformation. In-process displacement persists in the axial and radial directions from thermal expansion.



Temperature

Austenite Phase

Martensite Phase

Hoop Stress

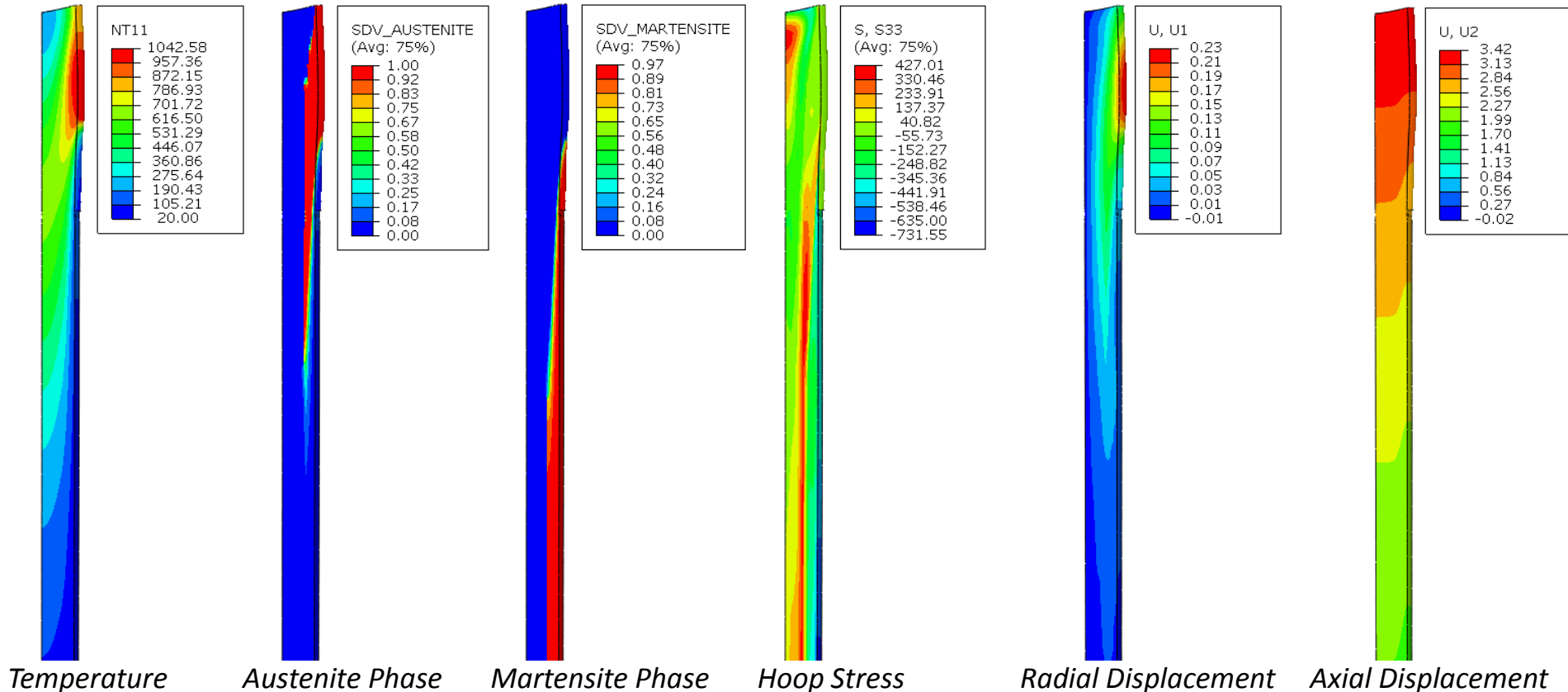
Radial Displacement

Axial Displacement

Stress, Phase and Displacement at Inductor Shutoff

Baseline - AISI 1541 – 25K W/(m²·°C) HTC

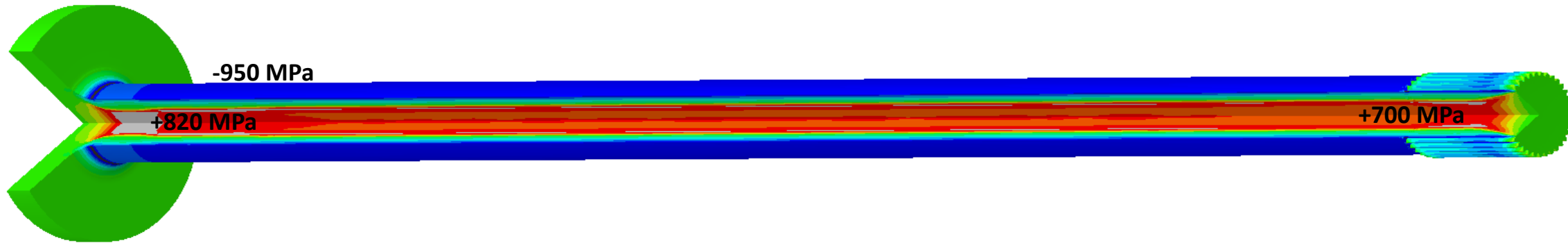
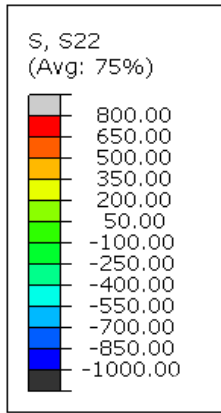
After 130.15 seconds of total process time, the inductor is shut off to prevent overheating of the spline end. A temperature of ~1040°C is shown in the spline tooth. Some of this heat will conduct to the core of the spline and slowly cool to pull the surface of this region into compression. The hoop stress contour shows surface compression in the fully transformed martensite region, with tension just under the hardened case. Axial displacement continues to grow, although some of this is residual thermal expansion, with the magnitude decreasing some as the part returns to thermal equilibrium.



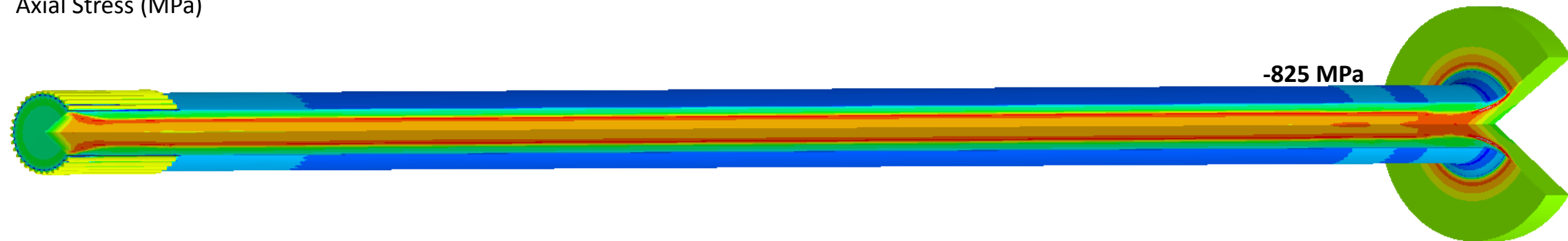
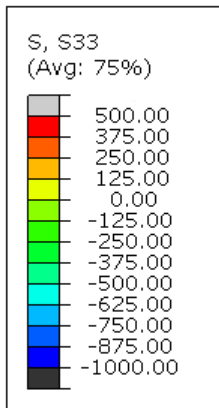
Residual Stress - End of Process

Baseline - AISI 1541 – 25K W/(m²·°C) HTC

Shown below is the final residual stress state of the baseline model. The Axial stress shows strong surface compression down the length of the shaft, with tension maximized just under the case and around the flange. Hoop stress results are similar to the Axial, showing surface compression and subsurface tension, although lower in magnitude when compared to the axial stresses.



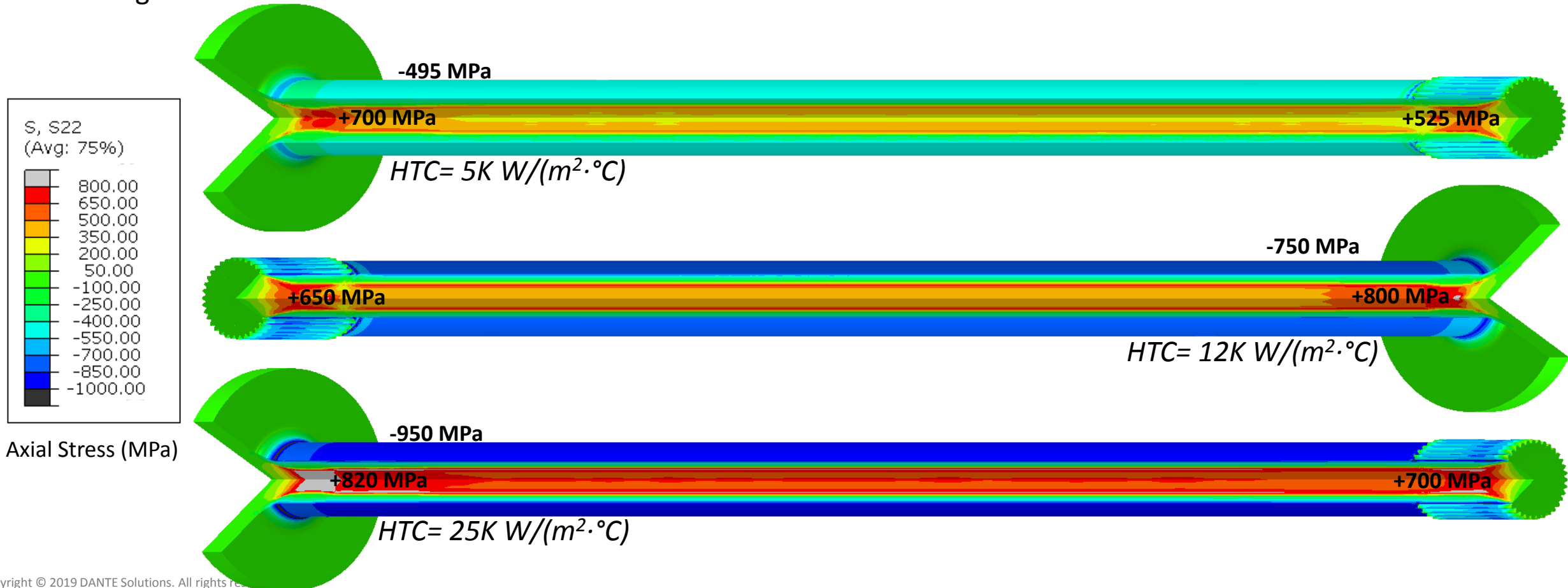
Axial Stress (MPa)



Hoop Stress (MPa)

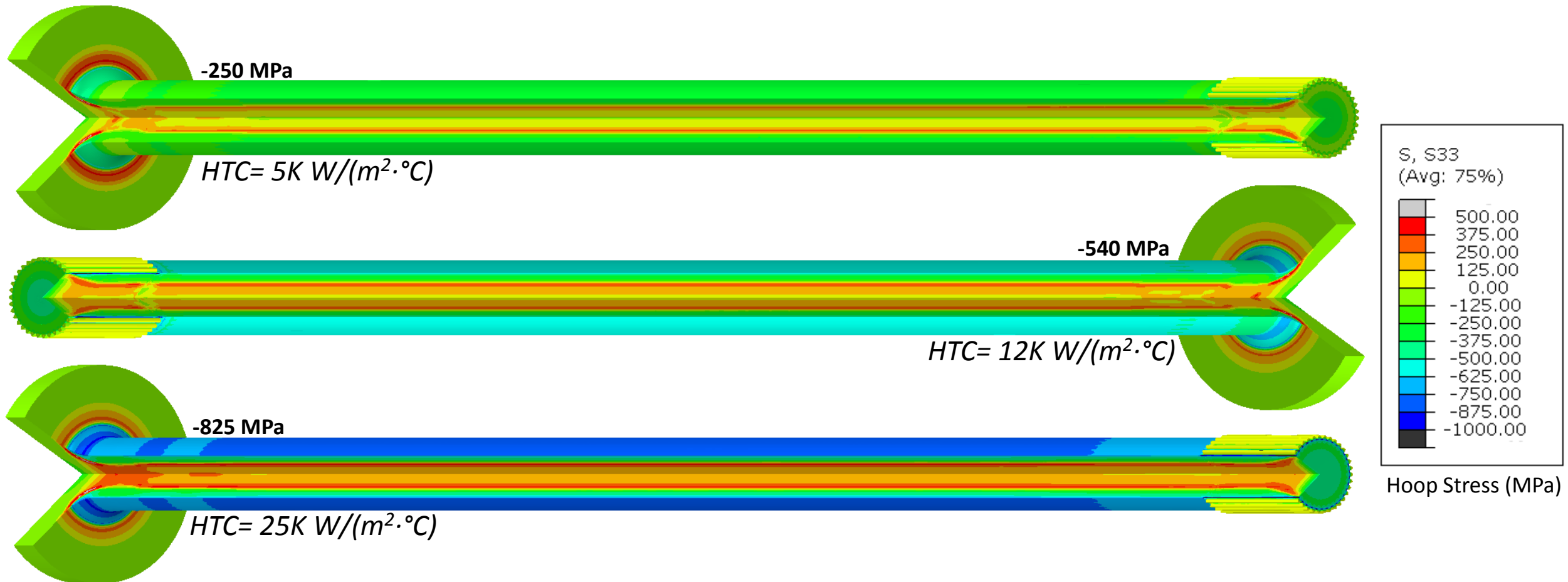
Effect of Varying Quench Rate (Axial Stress)

Applying three different quench rates; 5, 12, and 25 kW/(m²·°C), shows a dramatic change in residual stress. As the HTC increases, surface compression increases. To balance the increased surface compression, tensile stresses under the case also increase. The 25 KW/(m²·°C) quench HTC shows the desired highest surface compression, but some cause for concern persists in the magnitude of tension in the core by the flange. This may cause issues during loading and should be watched carefully for cracking or failure.



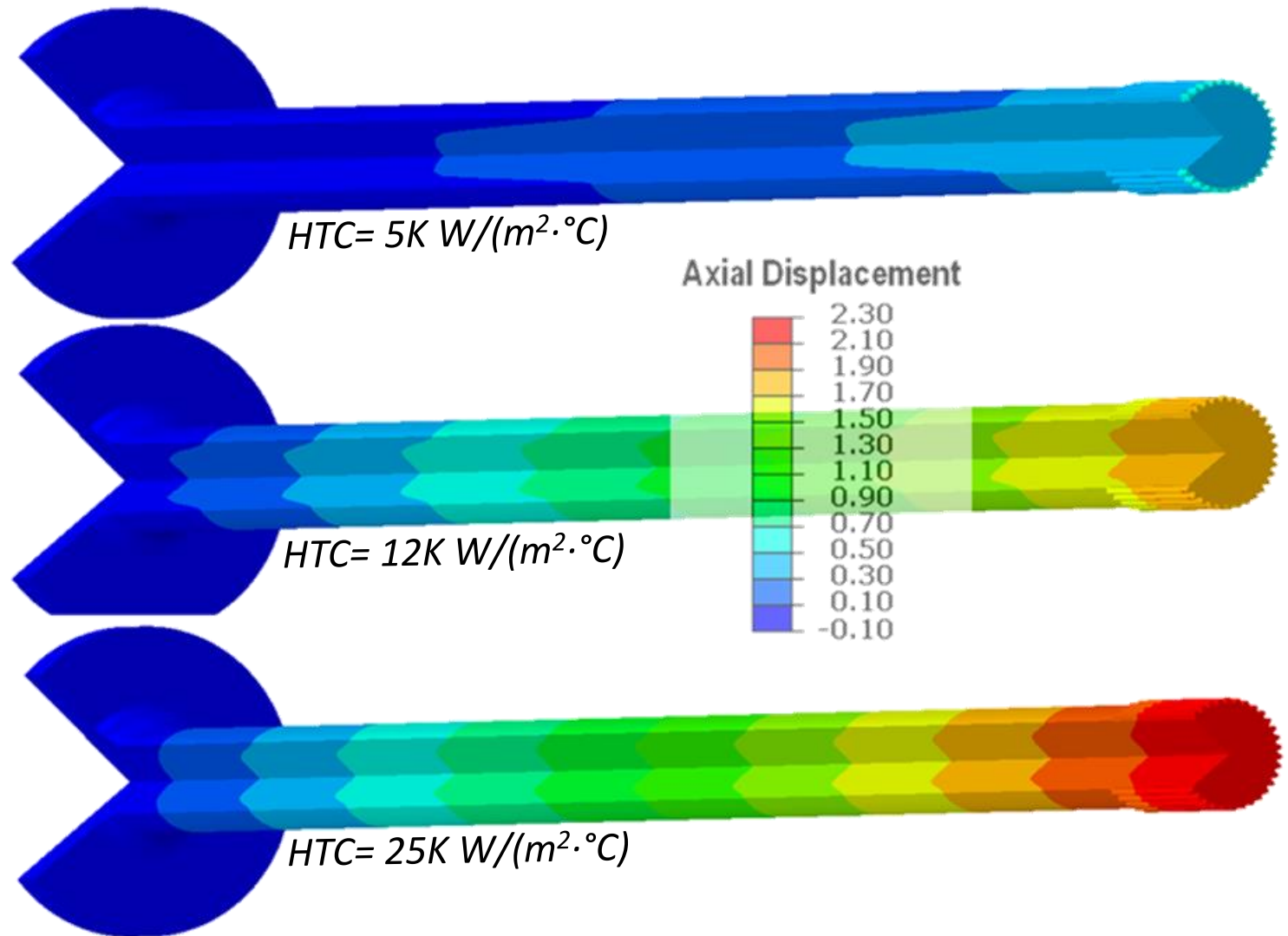
Effect of Varying Quench Rate (Hoop Stress)

Varying the quench rates has a very similar effect on residual hoop stress as it did with axial stress. As the quench HTC increases, the magnitude of surface compression increases. In the hoop direction, however, the magnitudes of tension in the core of the flange are not as concerning as they are in the axial direction.



Effect of Varying Quench Rate (Displacement)

Varying the quench HTC also has a significant effect on overall distortion of the shaft. The same legend is shown for all three quench rates, so the color difference represents the total magnitude of axial displacement. A higher cooling rate will result in a larger axial displacement. The 5K W/(m²·°C) quench rate model only elongated ~.3mm while the 25K W/(m²·°C) quench rate model elongated ~2.3mm from its original length. Using DANTE, these predicted elongations can be accounted for in the initial axle design in order to reduce waste and scrap.



Varying Material

The previous study focused on varying quench rates, with the same material; AISI 1541. This study focuses on material hardenability via chemistry to see the effect it has on residual stress. The two tables to the right show alloying element composition and martensite start temperatures (M_s) for AISI 1040, AISI 1541 and AISI 4140 grades of steel. All three grades of steel have similar carbon content, but differ in alloy content. These alloying elements will have an effect on phase transformation timing and depth of martensite formation.

Chemistries of Selected Alloys

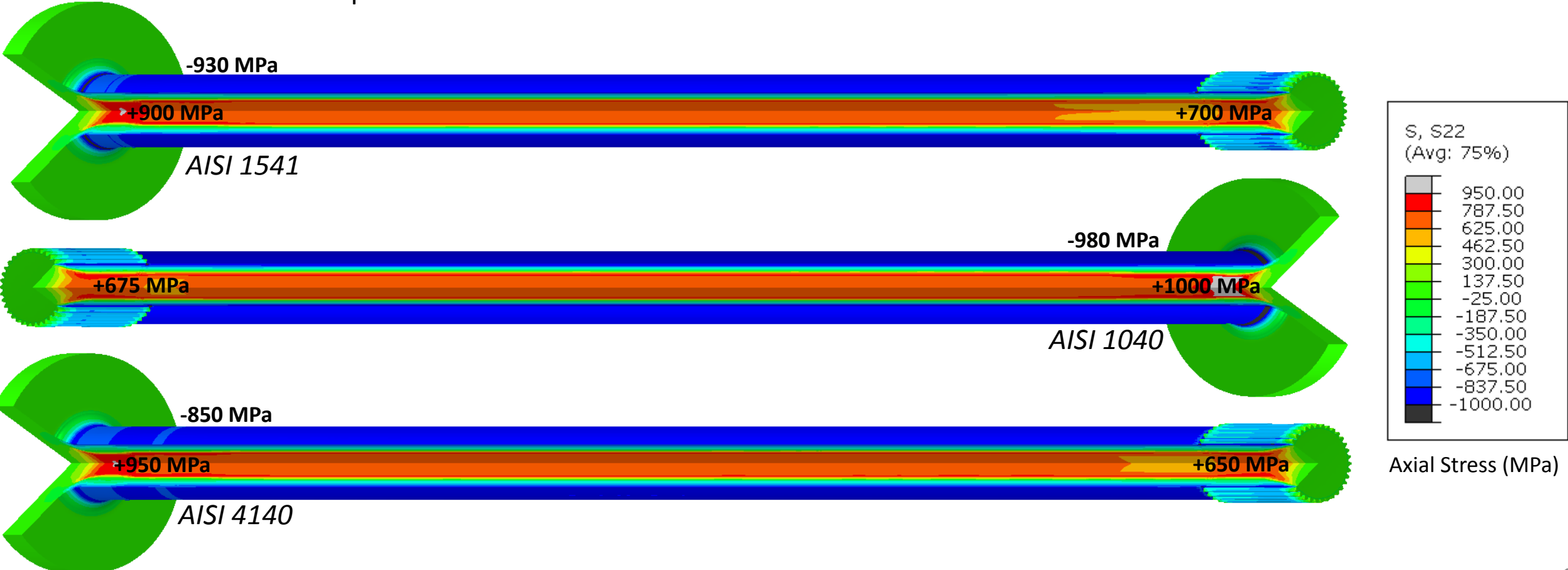
Alloy	C, w/o	Mn, w/o	Si, w/o	Cr, w/o	Ni, w/o	Mo, w/o	Fe
1040	0.4	0.75	0.2	0.05	0.05	-	Balance
1541	0.41	1.5	0.25	0.05	0.15	-	Balance
4140	0.4	0.87	0.25	0.95	0.15	0.2	Balance

Hardenability and Martensite Start Temperatures of Selected Alloys

Alloy	Calculated D_1 , mm	Martensite Start Temperature, °C
1040	29.9	306
1541	58.8	311
4140	129.2	327

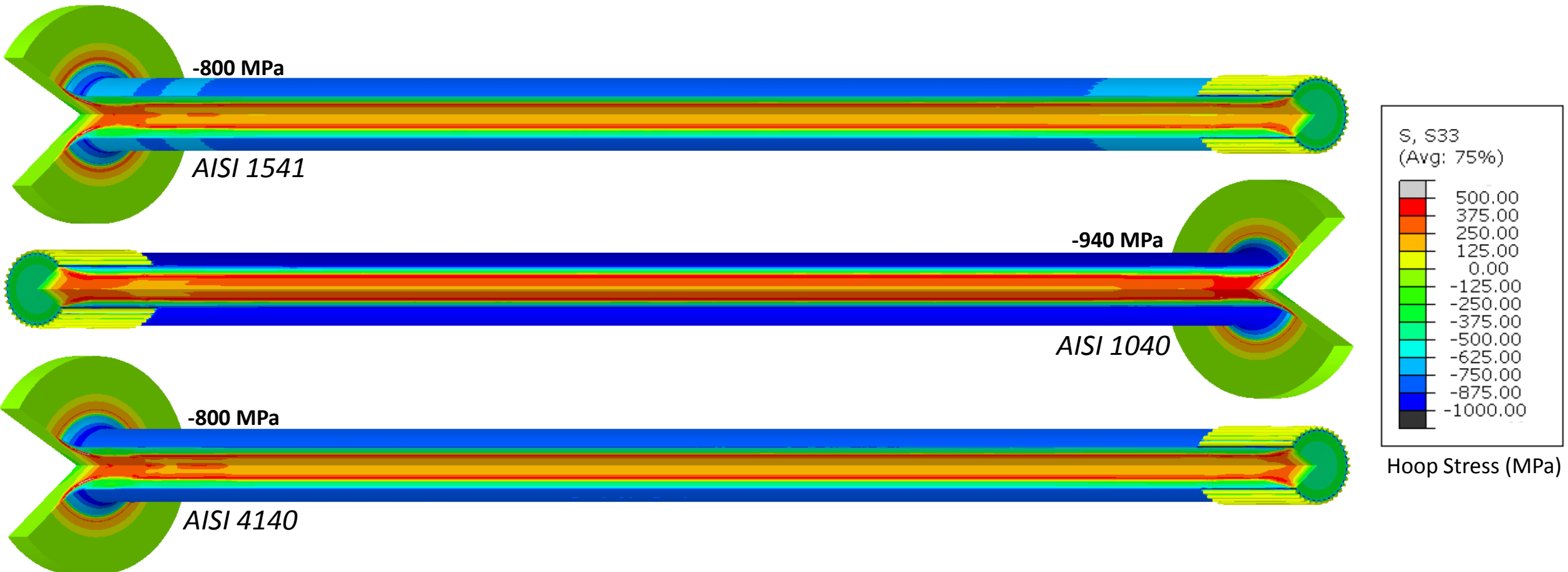
Effect of Varying Material (Axial Stress)

The residual stress contours of the three different steel grades shown below display a noticeable difference in axial stress. AISI 1040 shows the highest surface compression and highest core tension on the flange end. AISI 4140 shows the lowest surface compression overall, with core tensile values slightly higher than AISI 1541. The large magnitudes in AISI 1040 will be explored in future slides.



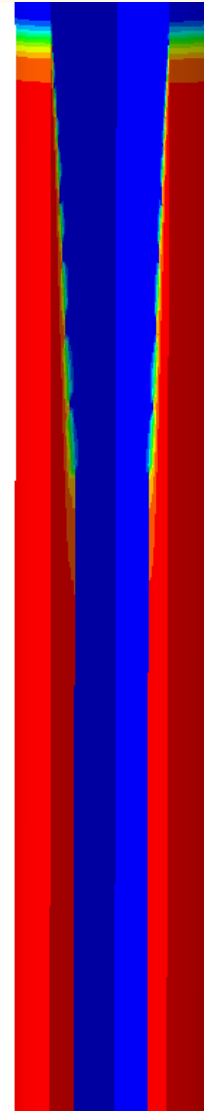
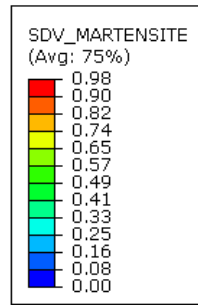
Effect of Varying Material (Hoop Stress)

The residual hoop stress contours below show similar findings to the axial stress contours. AISI 1040 continues to show the highest surface compression of all the materials. AISI 1541 and AISI 4140 show very similar magnitudes of hoop stress, although the distributions are slightly different.

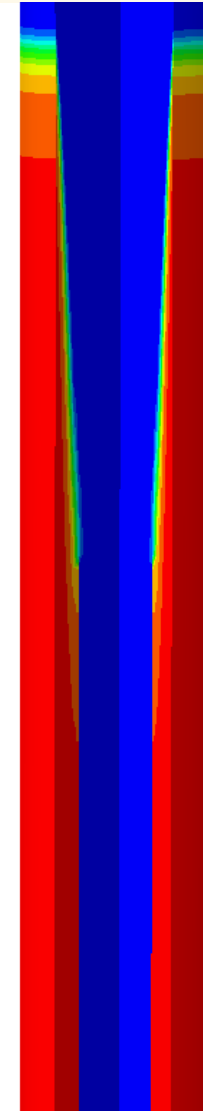


AISI 1040 Stress Factors

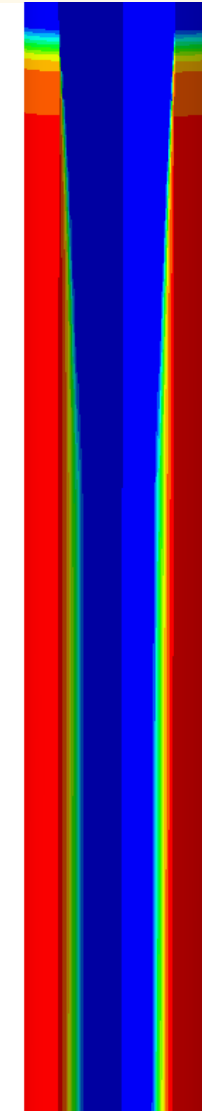
A closer look at the AISI 1040 model shows the cause of the much higher stress magnitudes. AISI 4140 and AISI 1541 have a higher hardenability than AISI 1040 due to their alloying content. This leads to a hardened case that is nearly all martensite. AISI 1040 has a martensitic surface and a bainitic subsurface. This variation in phase leads to a higher magnitude of residual compressive stress on the surface due to reduced subsurface volume expansion. Alternatively, AISI 4140 and AISI 1541 benefit from a subsurface martensite transformation that relieves some compression from the already transformed surface; in turn, reducing the level of tension in the core.



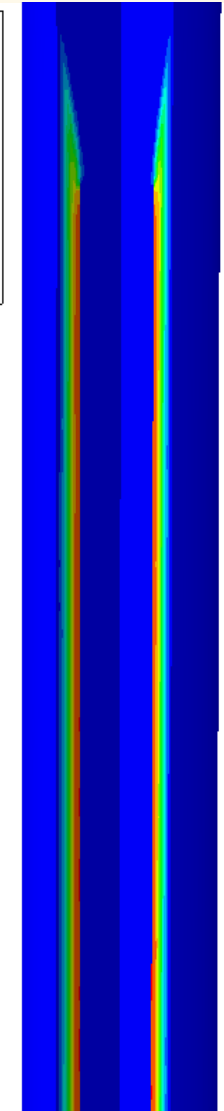
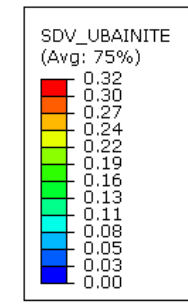
AISI 4140



AISI 1541



AISI 1040



AISI 1040 Bainite

Summary

Induction hardening processes offer a quick and effective solution to shaft hardening, but they also impart several sensitivities to the process:

- The heating rate, depth of heating, and total process time are all sensitive to frequency, power and the scan speed of the inductor. Modeling these parameters accurately is key to designing a desirable process.
- As the cooling rate is increased, a higher magnitude of surface compression is achieved. This subsequently leads to higher tension in the core, which may be problematic during service. A balance must be made in order to meet hardness and compressive stress requirements, while taking into account the residual tension and loading conditions the part will experience during service.
- Material hardenability plays a large role in the induction hardening sensitivities. Of the three materials modeled, the two with higher hardenability, AISI 1541 and AISI 4140, showed the most desirable final stress states. AISI 1040, on the other hand, showed that higher surface compressive stresses often lead to higher tensile stresses in the core. The phase transformation timing is often the largest contributing factor to the residual stress state.
- Heat treatment process modeling can help reduce quench cracks, reduce in-service failure, analyze service performance properties, and allow for an optimal design of the part and the process. Without modeling, the trial-and-error method would be costly and extremely time consuming.

Links to Relevant Case Study Material

Material related to this Case Study

[Scanning Induction Hardening of Truck Axle \(Poster\)](#)

[Effect of Spray Quenching Rate on Distortion and Residual Stresses during Induction Hardening of a Full-Float Truck Axle \(2013\)](#)

[Effect of Steel Hardenability on Stress Formation in an Induction Hardened Axle \(2015\)](#)

Additional DANTE Case Studies

<https://dante-solutions.com/case-studies>